



## Comparison Between Dimethoxy Chalcone and Its Dinitro Pyrazoline by Their Computational Prediction

SUBHA. R<sup>1</sup> and INGARSAL. N<sup>2\*</sup>

<sup>1,2\*</sup>PG & Research Department of Chemistry, Rajah Serfoji Government Arts College (Autonomous)  
(Affiliated to Bharathidasan University, Tiruchirapalli), Mayiladuthurai, TN, India.

\*Corresponding author E-mail: drningarsal@gmail.com

<http://dx.doi.org/10.13005/ojc/400418>

(Received: May 08, 2024; Accepted: August 13, 2024)

### ABSTRACT

Deriving a molecule (**1**) and its derivative (**2**) is the focus of the present study, and the different entities are to be compared and contrasted. Employing microwave as an assisting unit, the synthesis of (E)-3-(2,5-dimethoxy)-1-(4-methylthiophenyl)prop-2-en-1-one (**1**) was conducted using the relevant ketones and aldehydes. Starting from analogue (**1**), cyclization reaction by implementing the reflux method being used to yield pyrazoline derivative (**2**). These compounds underwent a preliminary characterization through IR spectroscopy. Together, the Auxiliary scans were performed spending the 6-311++G(d,p)/B3LYP method. Geometry of fully optimized structure with their binding informations, orbitals nature in molecules, electrostatic locations, values of dipole moments and atomic charges designed Mulliken's were anticipated. From these values, the reactive sites, molecules ability to accept or release a electron tendency, global descriptive parameters are noted. In addition to these studies, the pharmacokinetical behaviours are predicted by pkCSM and SwissADME tools. Further, the anti-inflammatory behaviour of molecules 1 and 2 are projected by molecular docking method with COX-II enzyme (pdb id : 3LN1). The docking interactions are better for both molecules and significantly important when compared with standard.

**Keywords:** Chalcone, Pyrazoline, DFT analysis, ADME-Tox prediction, Molecular Docking.

### INTRODUCTION

Chalcone and Pyrazoline moieties which include these, are a wider range of drugs that may be analogically, termed by two aspects: they are considered as biosynthetic chemicals on the one hand and as antifungal contours on the other. Chalcones are under research as wide as you can find applications in different areas including

anti-inflammatory, antifungal, antibacterial, antioxidant, antimalarial, antitumor agents<sup>1-9</sup>. Chalcones function as the both the donor and acceptor groups however, that makes them suitable for being investigated for their various uses in different fields. Derivatives of medical breakthroughs such as ibiza will be among the likely drugs. This is easier to imagine as an ibiza drug look alike will be similar to the chromatophore present in Ibiza (Ibiza



means "the colour of the sun") so that it can be used as a source of the sunscreen. Seasoning by the integrative organic conjugates is an abundance of optics and the computation characteristics that have been, at least, a focus of a lot of the studies of photonics, optoelectronics, integrated optics<sup>10,11</sup> and various high velocity applications, optic communication, storage and data processing. Their potential within NLO applications is outstanding, called that the inherent features of chalcones as NLO chromophores are excellent<sup>12</sup>. As a result of the mesoporous formulation, the eco-chalcones can go through charge transfer intermediate molecular mechanism, which implements the design principles of the system. For example, unlike cebelex, itaboloc and rimonabant, the central part of the molecules made from a pyrazole functions as a pyrazole. The pyrazole and its derivatives which are multi-functional biological elements in addition to its high selectivity are major factors that have provided this compound over the potential for the sustained synthetic research. Consequently, in addition to in-vitro bioactivity studies pyrazole molecules containing the donor and acceptor functional groups also have significant nonlinear optical characteristics<sup>13-15</sup>. The researcher performed the calculations by the DFand Nat. Bond Orbit. approach used for 1N-phenyl-3-(3,4-dichlorophenyl)-5-phenyl-2-pyrazoline, which are stated in literature<sup>16</sup>. The experiments and the theoretical calculations which Saminathan and his group members have done have led to the discovery for thiocyanooethanones pyrazoline joined<sup>17</sup>. Via this research, the structure and vibration frequencies have been determined. DFT calculations lead to the geometries and typical kinds of vibrations which are in decent contract with the experimentally observed data. The energies of HOMO-LUMO (Highest Occupied Molecular Orbital -Lowest Unoccupied Molecular Orbital) values of the molecules under study were calculated using a quantum mechanical method. We will be looking at the synthetic processes and structures of two homologous derivatives, both having donar or/and withdrawing groups. Predominantly of this category of molecules, scientists now detect the electronic structures and characteristics of the HOMO-LMO energies, MESP surface, dipolar moment, polarizable tendency, and the first hyperpolarizable values.

Besides inclusion of antimicrobial as well as ADME simulation and *in vitro* inflammatory experiments, we carried out the in silico study.

## EXPERIMENTAL

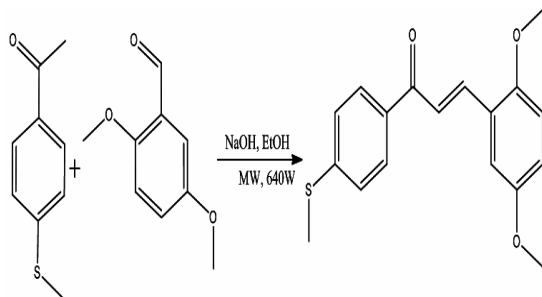
### MATERIAL AND METHODS

Of course, as a tentative we bought all chemicals commercially and without any preliminary purification. Open-capillary thermometers mounted without any hypothesis were used for the melting points. Variomicro V2.2.0 was used as automatic CHN analyzer. The spectrum of title substance was obtained by Shimadzu FT-IR in the range of 400-4000  $\text{cm}^{-1}$  using KBr disc as the method of analysis. The spectra were carried out with  $^1\text{H}$  and  $^{13}\text{C}$  nuclei proceeding a BRUKER (AVANCE III) 400MHz NMR spectrometer with DMSO as a solvent. These chemical shifts perceived are documented in on ppm for the shift. The main internal reference is the tetramethylsilane (TMS) which the NMR spectra are expressed through delta units (parts per million) with respect to standard. By dots, seperated, doublets, multiplets these  $^1\text{H}$  NMR signal preplanning can be noticed. FT-IR and NMR spectra were obtained from IACC associated with Chemistry Faculty, Gandhigram Rural Institute, Dindigul, Tamilnadu state.

#### Production of titled analogues

##### Production of (E)-3-(2,5-dimethoxyphenyl)-1-(4-methylthio)phenylprop-2-en-1-one (1)

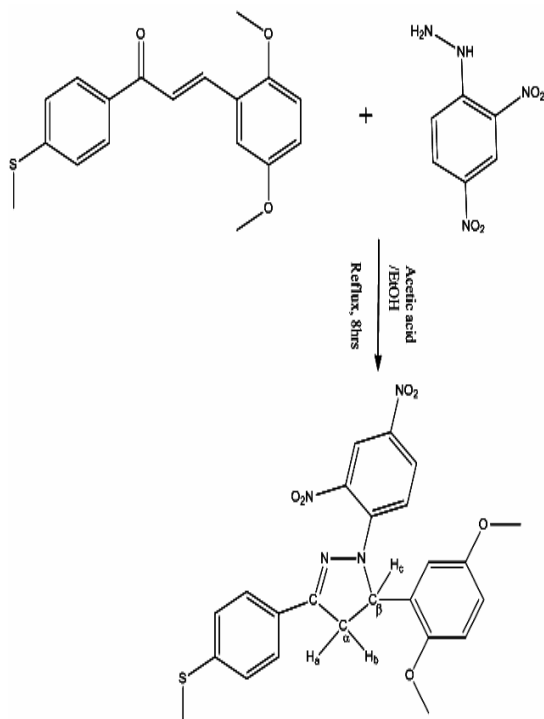
The described mole (2.5 mmol) of 1-(4-methylthio)ethanal and 2,5-dimethoxy benzaldehyde (2.5mmol) dissolved in 5 mL of absolute ethanol were added and the reaction blend was stirred with sodium hydroxide solution of 20 mmol (2 mL). In the next phase of this, I dip in microwave irradiation with 640W<sup>18</sup> for 2 min, by Scheme 1. The processing of production was watched by chromatographical method especially using thin-layer chromatogram (eluent 20:80: ethyl acetate: hexane). This part was followed via the neutralization reaction with the dilute HCL, then the product obtained through filtration and drying matched the desired one. Lastly, the purity of the final products recovered from such process was analyzed using absorption maximum (UV), FT-IR,  $^1\text{H}$  NMR,  $^{13}\text{C}$  NMR and MS analytical methods.



Scheme 1. Formation of chalcone moiety (1)

### Production of 5-(2,5-dimethoxyphenyl)-1-(2,4-dinitrophenyl)-3-(4-(methylthio)-phenyl)-4,5-dihydro-1H-pyrazole (2)

The mixture gradually added 1 (2.5mmol) as well as 2,4-dinitrophenylhydrazine (2.5mmol/15 mL) in ethanol, and then sodium acetate anhydrous (0.5 g) was refluxed<sup>19</sup> for 7-8 h (Scheme-2). Care is to be taken during the monitoring of the conversion to make sure all the initial reagent molecules have reacted. It was cooled quickly in addition to being discharged into water contains ice. The precipitate was filtered, dried and subjected to column n-hexane and ethyl acetate (3:1) as eluent. Eventually the product was re-crystallized using ethanol to get a solid pale yellow and glittering glitch. These give the spectral lines of the element and physical constants.



Scheme 2. Formation of substituted 1H-pyrazole (2)

### Studies by computation

As a result, the optimization of the geometry was achieved utilizing B3LYP functional within the B3LYP/6-311++G(d,p) level in the package of Gaussian09. The molecular polarizability values as well as hyper-polarizability values have been derived by the B3LYP/6-311++ G basis set along with the immobile basis set extrapolation method, whereas NBO designs were supported out with the B3LYP/6-311++G(d,p) premise set offered in Gaussian09.

## RESULTS AND DISCUSSION

### Spectral verification

Data on spectral and physical features of the synthesized analogues is narrated below.

#### Spectral scrutiny of (E)-3-(2,5-dimethoxyphenyl)-1-(4-(methylthio)phenyl)prop-2-en-1-one (1)

Molecular Formula:  $C_{18}H_{18}O_3S$ ; Yield: 81%; m.p. : 117-118°C; m/z 296; IR (KBr,  $\text{vcm}^{-1}$ ) 1650 (CO), 1215 ( $\text{CH}_{ip}$ ), 744 ( $\text{CH}_{op}$ ), 1037 ( $\text{CH}=\text{CH}_{op}$ ), 571 ( $\text{C}=\text{C}_{op}$ ).  $^1\text{H}$  NMR (400 MHz,  $\text{CDCl}_3$ ,  $\delta/\text{ppm}$ ) d 7.573(1H, d,  $J = 15.2$  Hz), 8.072 (1H, d,  $J = 15.5$  Hz), 6.857–7.959 (m, ArH), 3.814 (methyl);  $^{13}\text{C}$ -NMR (125 MHz,  $\text{CDCl}_3$ ,  $\delta/\text{ppm}$ ) 122.86 ( $\text{C}_\alpha$ ), 139.84 ( $\text{C}_\beta$ ), 189.76(CO), 112.48-153.524 (Ar. Carbons), 56.13 (methoxy), 14.84 (methyl); Elemental Analysis: Exp (%) : C : 68.76; H : 5.78; O : 15.27; S : 10.19; Cal (%) : C : 69.87; H : 4.71; O : 15.22; S : 10.17.

#### Spectral scrutiny of 5-(2,5-dimethoxyphenyl)-1-(2,4-dinitrophenyl)-3-(4-(methylthio)-phenyl)-4,5-dihydro-1H-pyrazole (2)

Molecular Formula:  $C_{24}H_{22}N_4O_6S$ ; Yield: 80%; m.p.: 188-189°C; IR  $\text{vcm}^{-1}$ : 2849 (CH str.), 1589 (C=N), 2918 (methylene str.), 1506 (Ar, C=C str);  $^1\text{H}$  NMR  $\delta(\text{ppm})$ : 3.35 ( $\text{H}_a$ , 1H-*dd*)ppm, 3.76 ( $\text{H}_b$ , 1H-*dd*)ppm, 5.26( $\text{H}_c$ , 1H-*t*)ppm, 6.85-7.36(m, Aryl protons)ppm,  $^{13}\text{C}$  NMR  $\delta(\text{ppm})$ :152.86(C=N)ppm, 40.80 ( $\text{C}_\alpha$ )ppm, 65.57( $\text{C}_\beta$ )ppm, 55.89(O- $\text{CH}_3$ )ppm, m.p. 131-132°C; Elemental Analysis : Exp (%) : C : 58.29; H : 4.48; N : 11.33; O : 19.41; S : 6.48; Cal (%) : C : 58.46; H : 4.38; N : 11.30; O : 19.36; S : 6.51.

### Optimization of compounds 1 and 2 geometries

By DFT method, the molecules 1 and 2 were optimized fully. The relevant structures are optimized of compounds 1 and 2 are presented in Figure 1.

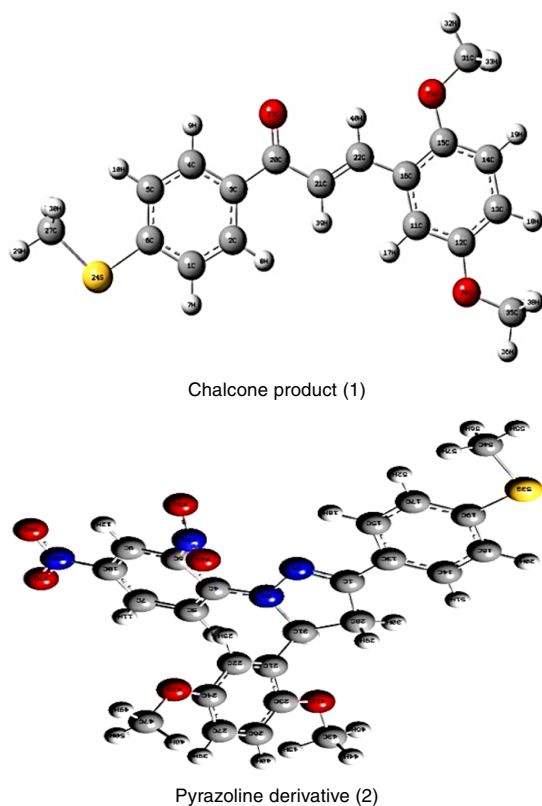


Fig. 1. Structures optimized by DFT of titled analogues 1 and 2

### Molecular orbital analysis

The MOs which are a clear function of the quantum mechanical factor are documented to be the major reactions and they are also used for depiction of kinetic stability, chemical reactivity, global softness, and hardness<sup>20,21</sup>. Thus, we carried out the molecular orbital analysis (HOMO-LUMO) to figure out their electron behavior as our molecular targets/compounds. The reality still exists; hence, we will be carrying out the HOMO-LUMO analysis by adhering the B3LYP/6-311++G(d,p) approach and in Table 1 are the results as you can see below. The plan of the said molecular orbitals were in Fig. 2. High position of orbital energy (HOMO) and low position of frontier orbital energy (LUMO) reflect the ability of compounds to that are good nucleophiles. Nucleophiles, in line with their properties which include electron pair sharing, do the donation as well. Anyway, a valid electrophilic compound has a low LUMO level of the matrix scale. Fig. 2, which brings the eyeballs to the space between molecules above LUMO (lowest unoccupied molecular orbital) is explained. In Fig. 2,

the energy information of HOMO (highest occupied electronic molecular orbital), LUMO (electronic least occupied molecular orbital) is given in Table 1. Meantime, the intramolecular charge-transfer (ICT) in organic compounds have the impact on the HOMO-LUMO energy gaps in Chalcone (3.576 eV) and Pyrazoline (2.258 eV). The inclusion of ICT properties strengthens HOMO-LUMO gaps in these chalcones compounds. Molecular conductivity depends on the band gap. Although the gap size allows not only quantitatively but also qualitatively accurate description of hardness, not reactivity is determined by conditional size. Energy gap HOMO-LUMO which is a measure of the compound's hardness is directly related to resulting energy difference. The size of the energy gap is the primary factor that determines the efforts involved in locating the target molecule. The theoretical values of electrochemical work functions can be obtained as a known fact.

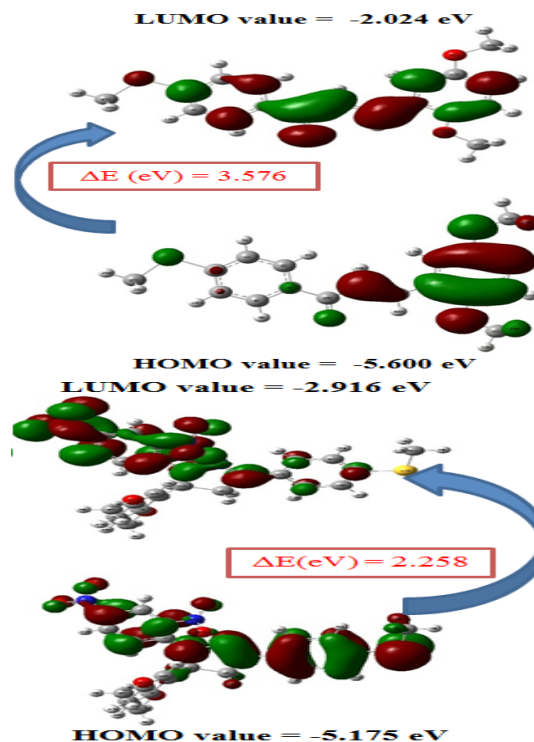


Fig. 2. Energies depicted from HOMO-LUMO's of compounds 1 and 2

The molecule 2 is more softness than 1 and it is expected to show higher biological behaviour for molecule 2.

**Table 1: Molecular orbital energies**

Factors	Values observed	
	Chalcone	Pyrazoline
HOMO-energy (a. u)	-5.600	-5.614
LUMO-energy (a.u)	-2.024	-2.720
HOMO-LUMO (a.u)	3.576	2.894
Ioniz. energy (I)	5.600	5.614
Elect. affinity (A)	2.024	2.720
Global stiffness ( $\eta$ )	1.788	1.447
Chem. potential ( $\mu$ )	-3.812	-4.167
Electrophilicity index ( $\omega$ )	4.064	6.001
Chemical smoothness (s)	0.559	0.691

### Dipole moment values

The dipolar moment is really decisive for molecular structural chemistry as an unambiguous confirmation that electronegativities occur among molecules throughout the molecule. This confirms that such a system is able to control the particular attribute of the molecule –ive. The orientational one that refers to the orientation of dipole moment vectors, thus when a positive charge point is found the other is negative. The dipole polar moment of Chalcone (1), which is estimated 4.615 D, is approximately 7.744 D with Pyrazoline (2). The relationship between the  $\% \alpha_0$  and  $\% \beta_{tot}$  density of the chemical or molecular dipole which dictates the structure directly indicates the nonlinear efficiency of optical molecules. In addition, the exhaustive search method with the table lets us perform an estimation of the  $\alpha_0$  and tot values (Table 2). Stronger  $\beta_{tot}$  of the pyrazoline as  $\text{NO}_2$  group donates the electron to the free electron negatively and weakens the electron flow in the compound.

The orbitals that have p character on the methyl group give rise to an adduct of methyl group which overlaps (with the accepting nitro group pi bond). However, these transitions of singlet and triplet to each other are additionally the reason for NLO properties that will be explained below. Such result is constructed on the power of the bond among molecules: the greater the number of molecules with carbonyl and nitro structure, the better are the NLO properties<sup>28</sup>. Hydrogen bondings evidently show the most strengths when it comes to the matter of those bonds (that is, for example, the energy of urea's  $\mu$  & are 1.3732 Debye and 0.03728 nanocoulomb each). Later on, for chalcones and pyrazoline, the polarizability of which molecule is situated,  $43.63 \times 10^{-24}$  and  $56.63 \times 10^{-24}$  esu as mean has been determined. The optimized version would lead to the

better NLO belongings that will have better success than urea even at a higher rate.

**Table 2: Parameters observed for NLO behavioural purpose through DFT way**

Factors	Symbol	Chalcone(1)	Pyrazoline(2)
Dipole moments	$\mu_{total}$	4.615D	10.844
Hyperpolarizability	$\beta_0$	$2.263 \times 10^{-30}$ esu	4.195
Polarizability	$\alpha_0$	$19.007 \times 10^{-24}$ esu	30.794

### Molecular surfaces

The Molecular Electrostatic potential (MESP) is one of the methods that may serve as a guide mapping the shades of interactions that exists in molecules and in the case of intermolecular interactions. They may also be used for the further prediction of reactive spots and relative reactivity towards an electrophilic attack. Moreover, it hand over a locations measurement of compounds 1 and 2 for their either electrophilic or nucleophilic attack by applying the B3LYP/6-31G (d, p) level. In the MEP diagram, the couple of negative sections (red and yellow) are defining the electrophilic reactants, and the positive region (where the axis pass through) indicates the nucleophilic one. For lucidity, the color of the MESP outward is as follows: In easily comprehensible manner, red spots are the electron deficient areas on the molecule that are negatively charged. The blue indicates, there is the deficiency of electrons in the atmosphere of molecule, but it is partially electron negative; in contrast, the blue light is devoid of electron presence, and there is a presence of medium amount of electron on the yellow part. However, the green is near to the neutral condition in terms strengthening the negative charge and there is mainly found at the oxygen atoms in nitro and carbonyl group and this provides the principal sites for electrophilic attack at these nominated points. Important positive site is a non-bonding electron shared by hydrogen atom of H-C=C-H group which is likely also a nucleophile addition site. Here is where molecules manifest the intermolecular interactions of say, forces of attraction (or not). Likewise, the presence intersystem C-H- $\pi$  - $\pi$  interactions in solid state for the chalcone is also approved by NMR. Both pyrazoline nitrogen and atomic oxygen of the nitro group react rapidly to the electrophilic sites.

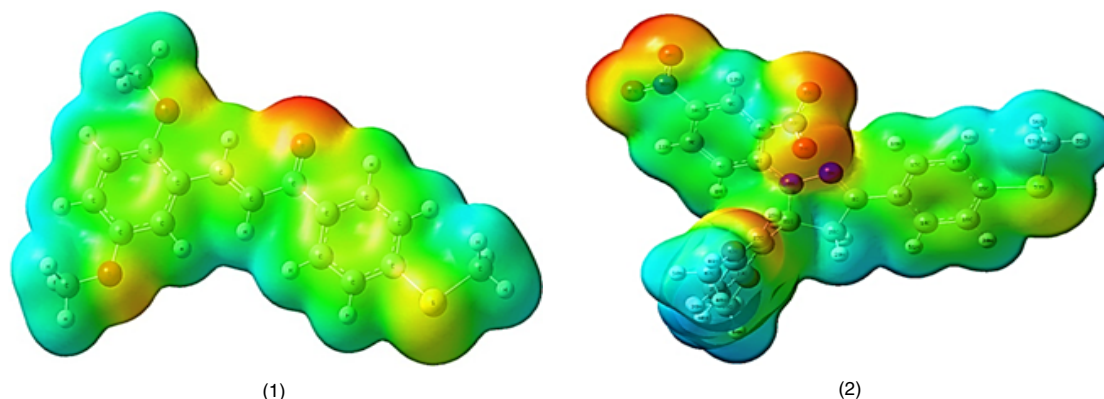


Fig. 3. MEP illustration of analogues 1 and 2

### Atomic Charges by Mulliken

Simplified atomic charges by Mulliken can be observed in Table 3 on the following page. The concept of Mulliken atomic charge calculation is vital<sup>30,31</sup> in the sphere of quantum chemistry calculations. The Table 3 elucidates that the carbonyl carbons C7 (0.262), sulphur atom S4 (0.271), and methoxy carbons 12C' (0.293) and 15C' (0.268) are most positive charges specifically C7 atoms, this is also a site for nucleophilic attack in the Chalcone (1). Considering pyrazoline structure, sulphur S9 (0.300), C18 (0.452), and C21 (0.315) atoms may be effective sites of attacks by electrophile due to larger values. The atoms of oxygen attached to the carbonyl group C=O10 (-0.444) but also the group of methoxy oxygens by O12 (-0.536) and O15 (-0.538) have shown the most negative charge in the chalcones and then to the pyrazoline nitrogens by N1 (-0.601), N2 (-0.203). These findings then showed that these sites were capable of accepting extra negative charge; they were thus good nucleophilic

sites. Such display of data is represented as Figure 4.

### Pharmokinetic predictions for compounds (1) and (2)

In Table 4, the elements, weights and their other predictions are displayed. Without doubt, it supports that they followed the Lipinski's Rule of 5 and may be beneficial for other drug analysis procedure<sup>32</sup>. The solubility of the compound 1 is greater than 2, while both present good intestinal absorption values. Besides, the two are non Pgp substrates and they experience no effect in absorption. Molecule 2 has been found to be 100% of PPB value which demonstrated its great penetrating ability of drug. The noncompetitive CYP2D6 and CYP3A4 inhibitors exhibited a good metabolic property<sup>33</sup>. The clearance values recommended that the drug is mostly removed from the body. They are also non-toxic. In sum, both molecule 1 and 2 are possible to test using an *in-vitro* method for further biological studies.

Table 3: Atomic charges (Mulliken's) of analogues 1 and 2

Chalcone analogue (1)				Pyrazoline analogue (2)			
Atom number and type	Charge	Atom number and type	Charge	Atom number and type	Charge	Atom number and type	Charge
1 C	0.027	10 O	-0.444	1 N	-0.601	15 C	-0.002
2 C	0.020	11 C	0.049	2 N	-0.203	16 C	-0.009
3 C	0.032	12 C	0.225	3 C	0.175	17 C	0.261
4 C	-0.279	12 O	-0.536	4 C	0.025	17 O	-0.581
4 S	0.271	12 C'	0.293	5 C	0.195	18 C	0.452
4 C'	-0.089	13 C	-0.005	6 C	0.090	19 C	0.252
5 C	0.038	14 C	0.029	7 C	0.068	19 N	0.068
6 C	0.050	15 C	0.223	8 C	-0.007	19 O	-0.279
7 C	0.262	15 O	-0.538	9 C	-0.223	20 C	0.125
8 C	-0.006	15 C'	0.268	9 S	0.300	21 C	0.315
9 C	0.105	16 C	0.006	10 C	-0.004	21 N	0.031
				11 C	-0.005	21 O	-0.305
				12 C	0.069	22 C	0.083
				13 C	0.023	23 C	-0.004
				14 C	0.284	14' C	0.301
				14 O	-0.557	17' C	0.310

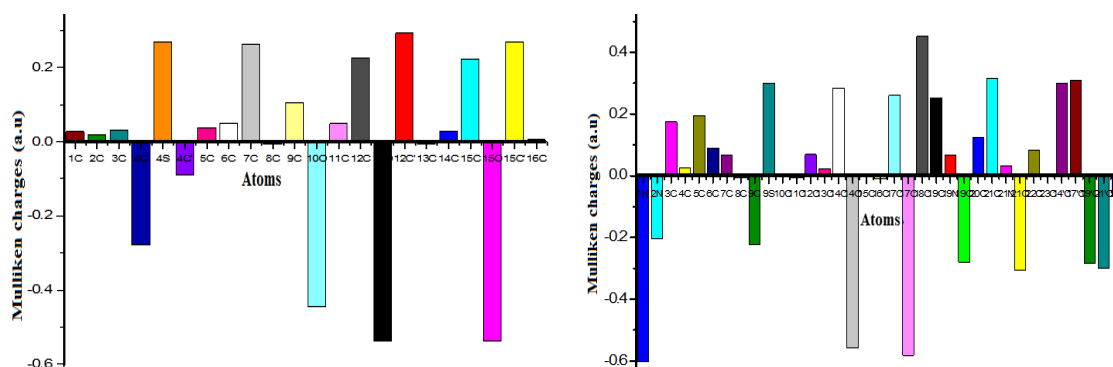


Fig. 4. Diagram of mulliken's charges for 1 and 2

Table 4: Pharmacokinetic and ADMET parameters of molecules (1) and (2)

Molecule	DRUGLIKENESS	
	1	2
Mol. Formula	C <sub>18</sub> H <sub>18</sub> O <sub>3</sub> S	C <sub>24</sub> H <sub>22</sub> N <sub>4</sub> O <sub>6</sub> S
Ml. Wt	314	494
No. of atoms	22	35
No. of Rotatable bonds	6	8
No. of H-bond acceptors	3	8
No. of H-bond contributors	0	0
ClogP	3.46	3.36
Lipinski's Rule of 5	No violation	No violation
	(A) ABSORPTION	
Water Solubility (Log S)	-4.41	-6.217
MR	90.95	144.61
Skin Permeability (log Kp)	-2.399	-2.24
Caco-2 permeability	55.4982	0.441
Human intestinal absorption (HIA)	97.556125	100
PPB	96.898031	100
Pgp substrate	No	No
	(D) DISTRIBUTION	
VDss (human)	0.587	0.724
Fraction unbound (human)	0	0
Blood-brain barrier permeability	0.148	0.416
CNS permeability	-1.458	-1.389
	(M) METABOLISM	
CYP3A4 substrate	Yes	Yes
Inhibition of CY-P2D6 enzyme	No	No
Inhibition of CY-P3A4 enzyme	No	No
	(E) EXCRETION	
Total drug Clearance	0.151	-0.077
Renal OCT-2 substrate	Yes	Yes
	(T) TOXICITY	
AMES tox	No	No
Hepatotoxicity	No	No
hERG I inhibitor	No	No
hERG II inhibitor	No	No

### Molecular Dcking of 1 and 2 with COX-II enzyme (pdb id: 3In1)

Molecular docking of compound 1 and 2 using Auto dock vina is done and visualization with Biovia DS visualizer is performed. Both of the molecules are found to have a good affinity,

better than standard drug. In addition, 1 and 2 have exhibited good H-bonded interactions with ligand selected. We observed both the molecules 1 and 2 forming three number of conventional bonds with short distances which are much more active than standard. Carbonyl oxygen and



nitro oxygen made strong interactions and this, in turn, facilitate the inhibition. In addition to these, some other interactions also increased the molecular docking as a good inhibitory function. The obtained results are indicated in the Table 5.

The conventional and hydrophobic interactions of molecules **1** and **2** with receptor protein are visualized in Biovia Discovery Studio Visualizer. In Fig. 5, the docking pose of ligands surrounded by the protein surfaces are given as 3D view and type of interacting nature is given in 2D view.

**Table 5: Molecular docking interactons of compounds 1 and 2 with COX-II enzyme receptors**

Ligand Compounds	Binding energy kcal/mol	No. of interactions	Hydrogen Bonding interactions		Hydrophobic interactions Amino acid residue
			Amino acid residue	No. of interactions	
1	-8.4	3	ASN368 (2.0166Å°), GLN275 (2.0689Å°) & GLU276 (3.7544Å°)	Others-1, Hydrophobic-5	Pi-Sulfur (HIS193); Pi-Pi Stacked (HIS193 & HIS372); Pi-Alkyl (HIS 193, HIS374 & VAL277
2	-8.3	3	ASN368 (1.7786Å°), THR198 (2.5886Å°) & TYR134 (2.7462Å°)	Hydrophobic-6, Others-1	Pi-Sulfur (PHE390); Pi-Pi T-shaped (HIS200); Alkyl (VAL277, VAL281 & LEU377); Pi-Alkyl (HIS193); Pi-Sulphur (PHE390)
Dichlofenac Sodium (STD)	-9.2	2	ARG106-HH22 (2.6455Å°) & ARG106-HH12 (2.7038Å°)	Hydrophobic-7, Others-1	Pi-sigma (VAL509); Amide-Pi Stacked (GLY512 & ALA513); Alkyl (VAL335 & MET508); Pi-Alkyl (PHE504, LE338 & ALA513) & Electrostatic (ARG106)

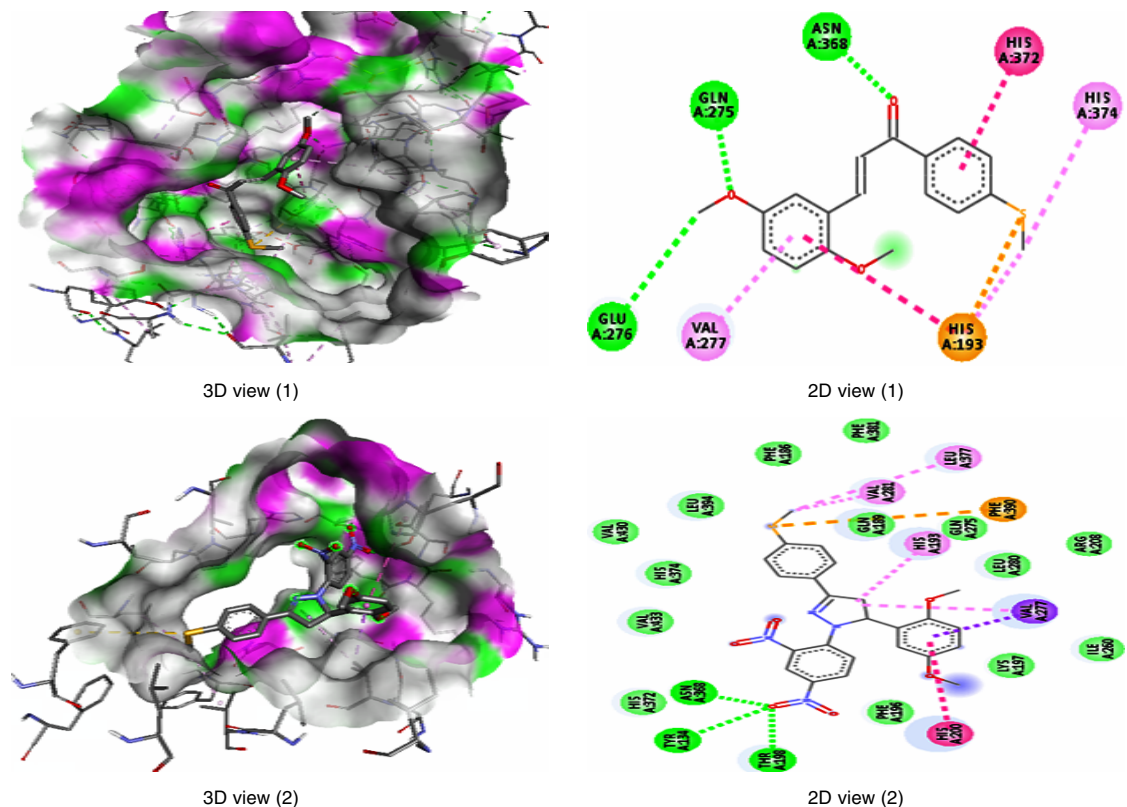


**Fig. 5. 3D and 2D view interactions of molecules with receptor**



## CONCLUSION

Here, a novel diaryl propenone (**1**) and its cyclic 2-pyrazoline (**2**) were obtained by proper methods. Functional stretches are revealed by IR and position & numbers of protons, carbons are recognized by respective NMR technique. The bonding lengths, angles are considered by DFT using Gaussian 09W programme. Also, electron transition tendencies are focused by FMO energies, MESP performances and atomic charges depicted by Mulliken were designed. The differences in HOMO-LUMO gap energy assumed that analogue (**2**) is more sensitive and soft than analogue (**1**). The dipolar tendencies also publicized that compound (**2**) has decent NLO stuff. Both the molecules obeyed the Lipink's rule without any destruction and so they may fit for drug analysis.

Further, the molecular docking of compounds **1** and **2** with COX-II enzyme revealed good inhibitory property especially, the carbonyl and nitro oxygens interacted with enzyme more closely and involved strong conventional interactions.

## ACKNOWLEDGEMENT

We show gratitude to our PG Department (Chemistry) for providing research facility, DG Govt. Arts College (women), Mayiladuthurai to exploit this effort.

## Conflict of interest

It is declared that there are no known competing financial interests for author and also declared there is no personal relations to inspiration the work conveyed in this research.

## REFERENCE

- Damodar, K.; Kim, J.-K.; Jun, J.G., *Chin. Chem. Lett.*, **2016**, *27*(5), 698–702.
- Vembu, S.; Pazhamalai, S.; Gopalakrishnan, M., *Med. Chem. Res.*, **2016**, *25*(9), 1916–1924.
- Sivakumar, P. M.; Muthu Kumar, T. M.; Doble, M., *Chem. Biol. Drug Des.*, **2009**, *74*(1), 68–79.
- Muškinja, J.; Burmudžija, A.; Ratković, Z.; Ranković, B.; Kosačić, M.; Bogdanović, G. A.; Novaković, S. B., *Med. Chem. Res.*, **2016**, *25*(9), 1744–1753.
- Mazzone, G.; Galano, A.; Alvarez-Idaboy, J. R.; Russo, N., *J. Chem. Inf. Model.*, **2016**, *56*(4), 662–670.
- Tadigoppula, N.; Korthikunta, V.; Gupta, S.; Kancharla, P.; Khaliq, T.; Soni, A.; Srivastava, R. K.; Srivastava, K.; Puri, S. K.; Raju, K. S. R., *J. Med. Chem.*, **2012**, *56*, 31–45.
- Sharma, N.; Mohanakrishnan, D.; Sharma, U. K.; Kumar, R.; Sinha, A. K.; Sahal, D., *Eur. J. Med. Chem.*, **2014**, *79*, 350–368.
- Pingaew, R.; Saekee, A.; Mandi, P.; Nantasenammat, C.; Prachayasittikul, S.; Ruchirawat, S.; Prachayasittikul, V., *Eur. J. Med. Chem.*, **2014**, *85*, 65–76.
- Cabrera, M.; Simoens, M.; Falchi, G.; Lavaggi, M. L.; Piro, O. E.; Castellano, E. E.; Vidal, A.; Azqueta, A.; Monge, A.; De Ceráin, A. L.; Sagrera, G.; Seoane, G.; Cerecetto, H.; González, M., *Bioorg. Med. Chem.*, **2007**, *15*(10), 3356–3367.
- Coskun, D.; Gunduz, B.; Coskun, M. F., *J. Mol. Str.*, **2019**, *1178*, 261–267.
- Hegde, H.; Sinha, R. K.; Kulkarni, S. D.; Shetty, N. S., *J. Photochem. & Photobiol. Chem.*, **2020**, *389*, 112222.
- Aboelnaga, A.; Mansour, E.; Ahmed, Hoda. A.; Hagar, M., *J. Kor. Chem. Soc.*, **2021**, *65*(2), 113–120.
- Viana, G. S. B.; Bandeira, M. A. M.; Matos, F. J. A., *Phytomed.*, **2003**, *10*(2–3), 189–195.
- Wu, X.; Tiekink, E. R. T.; Kostetski, I.; Kocherginsky, N.; Tan, A. L. C.; Khoo, S. B.; Wilairat, P.; Go, M.-L., *Eur. J. Pharm. Sci.*, **2006**, *27*(2–3), 175–187.
- Luo, Y.; Song, R.; Li, Y.; Zhang, S.; Liu, Z.-J.; Fu, J.; Zhu, H.-L., *Bioorg. Med. Chem. Lett.*, **2012**, *22*(9), 3039–3043.
- Anto, R. J.; Sukumaran, K.; Kuttan, G.; Rao, M. N. A.; Subbaraju, V.; Kuttan, R., *Canc. Lett.*, **1995**, *97*(1), 33–37.
- Saminathan, M.; Kanagarajan, S.; Chandrasekaran, R.; Sivasubramaniyan, A.; Raja, R.; Alagusundaram, P., *J. Chin. Chem. Soc.*, **2020**, *67*(6), 1100–1112.
- Unchadkar, A.; Zangade, S.; Shinde, A.; Deshpande, M., *J. Turkish. Che. Soc.*, **2015**, *2*(1)A, 1-8.
- Patel, N. B.; Shaikh, F. M.; Patel, H. R.; Rajani, D., *J. Saudi Chem. Soc.*, **2016**, *20*, S451-S456.
- Omri, N.; Yahyaoui, M.; Banani, R.; Messaoudi, S.; Moussa, F.; Abderrabba, M., *J. Theor. Comput. Chem.*, **2016**, *15*(01), 1650006.

21. Kosar, B.; Albayrak, C., *Spectrochim Acta. Mol. & Biomol. Spectr.*, **2011**, *78A*(1), 160-167.
22. Mishra, R.; Srivastava, A.; Sharma, A.; Tandon, P.; Baraldi, C.; Gamberini, M. C., *Spectrochim. Acta. Mol. Biomol. Spectr.*, **2013**, *101A*, 335–342.
23. Parr, R. G.; Szentpály, L. V.; Liu, S., *J. Am. Chem. Soc.*, **1999**, *121*(9), 1922–1924.
24. Parr, R. G.; Donnelly, R. A.; Levy, M.; Palke, W. E., *J. Chem. Phys.*, **1978**, *68*(8), 3801–3807.
25. Chattaraj, P. K.; Roy, D. R. Update 1 of: *Chem. Rev.*, **2007**, *107*(9), PR46–PR74.
26. Lesar, A.; Milošev, I., *Chem. Phys. Lett.*, **2009**, *483*(4–6), 198–203.
27. Sheela, N. R.; Muthu, S.; Sampathkrishnan, S., *Spectrochim. Acta. Mol. & Biomol. Spectr.*, **2014**, *120A*, 237–251.
28. Marchewka, M. K.; Baran, J.; Pietraszko, A.; Haznar, A.; Debrus, S.; Ratajczak, H., *Solid State Sci.*, **2003**, *5*(3), 509–518.
29. Qudar, J. L.; Hierle, R., *J. Appl. Phys.*, **1977**, *48*(7), 2699–2704.
30. Govindarajan, M.; Karabacak, M.; Suvitha, A.; Periandy, S., *Spectrochim. Acta. Mol. & Biomol. Spectr.*, **2012**, *89A*, 137–148.
31. Gunasekaran, S.; Kumaresan, S.; Arunbalaji, R.; Anand, G.; Srinivasan, S., *J. Chem. Sci.*, **2008**, *120*(3), 315–324.
32. Lipinski, C. A., *Drug Today Technol.*, **2004**, *1*(4), 337–341.
33. Ibrahim, Z. Y.; Uzairu, A.; Shallangwa, G.; Abechi, S., *Sci. Afr.*, **2020**, *10*, e00570.
34. Bharathi, R.; Santhi, N.; *J. Biotechnol. Bioinforma Res.*, **2021**, *3*(2), 1–6.